

# Effects of the Recess Length of a Coaxial Injector on a Transcritical $\text{LO}_2/\text{H}_2$ Jet Flame

A. Ruiz<sup>1</sup>, T. Schmitt<sup>2</sup>, L. Selle<sup>3</sup>, B. Cuenot<sup>1</sup> and T. Poinso<sup>3</sup>

<sup>1</sup> CERFACS, 52 avenue G. Coriolis, 31057 Toulouse Cedex, France

<sup>2</sup> EM2C, CNRS and Ecole Centrale Paris, 92295 Chtenay-Malabry, France

<sup>3</sup> IMFT, Avenue C. Soulas, 31400 Toulouse, France

## 1 Introduction

Nowadays, hard competition between aerospace manufacturers calls for the development of innovative systems, implying long and costly studies [1]. In rocket propulsion using liquid propellants, the combustion chamber is one of the key elements. If not designed properly, safety issues can occur, when high-frequency instabilities develop in the combustion chamber and provoke structural damage to the whole system. This phenomenon is particularly difficult to study experimentally, due to the high cost of the tests. Moreover, the power required for hot fire tests of rocket elements is so large that sometimes no experimental test rig can supply it.

In a  $\text{LO}_2/\text{H}_2$  rocket engine at nominal operating conditions, the combustion chamber pressure (typically around 10 MPa) is above the critical point of both reactants while the oxygen is injected in a liquid-like state, at a subcritical temperature ( $\sim 100$  K). This particular injection mode is designated as “transcritical”. The combustion physics of a transcritical flow is totally different from atmospheric conditions. In a typical coaxial injector configuration, below the critical pressure, the central liquid oxygen jet is atomized, due to shear stress induced by the surrounding high-speed gaseous hydrogen jet. Droplets and ligaments are formed around the  $\text{LO}_2$  jet due to surface tension. They vaporize as they come close to the reaction zone and gaseous  $\text{O}_2$  burns with gaseous  $\text{H}_2$ . Above the critical pressure, surface tension and latent heat of vaporization vanish. Experimental observations show that droplets and ligaments are replaced by “comb-like” structures and that the change of density takes place in the absence of a liquid-gas interface [2–4]. As a consequence, mass transfer from the  $\text{LO}_2$  and gaseous hydrogen streams towards the reaction zone is mainly controlled by turbulent diffusion (see [5] for a review of the physical phenomena).

Because of the difficulties of experimental studies, Computational Fluid Dynamics (CFD) has been used for decades in the development of rocket propulsion systems. Traditionally, the Reynolds Averaged Navier-Stokes (RANS) method for predicting the turbulent reacting flow inside the combustion chamber [6–8] is used by aerospace manufacturers to carry out parametric studies around a given design, and determine the most promising design before undertaking hot fire tests. However, the predictive capability of the RANS method for new designs is limited. Moreover, it is not able to describe unsteady phenomena like combustion and hydrodynamic instabilities or unsteady heat transfer.

To address these problems, Large-Eddy Simulations (LES) of turbulent transcritical flows have recently been undertaken. First studies focused on the near vicinity of coaxial injectors [9–11]. The AVBP LES code used in the present study, has already been successfully applied to various turbulent flows: a non reactive nitrogen transcritical injection [12], a transcritical  $\text{LO}_2/\text{H}_2$  flame [13] and a transcritical  $\text{LO}_2$ /methane flame [14], from the injection unit to the flame termination. These studies have shown the ability of LES to capture the correct physics in unsteady transcritical flows.

In the present paper, the LES technique is used to analyse the effect of a critical design parameter on the flame characteristics. Indeed, preliminary test have shown that the recess length of the  $\text{LO}_2$  post from the  $\text{H}_2$  post, as represented on Figure 1, have a great influence on the system behaviour. There is experimental evidence that the increase in recess length triggers an hydrodynamic instability that interacts with the flame and changes its shape and length [15]. The configuration used herein represents the unsteady turbulent reactive flow in a laboratory-scale combustion chamber, using a single-element coaxial  $\text{LO}_2/\text{H}_2$  injector with and without recess, at operating conditions close to a cryogenic liquid rocket engine at the nominal point. In the litterature, subcritical-pressure two-phase flow simulations using LES [16] have enabled to understand the link between the recessed length and the hydrodynamic instability. The ultimate goal of the present study is to predict the development of this instability along with the whole turbulent reactive supercritical field.

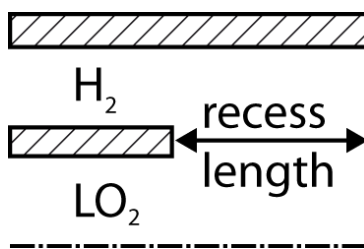


Figure 1: Recess length of the  $\text{LO}_2$  post from the  $\text{H}_2$  post

## 2 Description of the LES Solver

The AVBP code [17–19] used herein solves the 3D Navier-Stokes compressible equations, for reactive flows. It is massively parallel and uses unstructured grids, for a good description of complex geometries. The numerical scheme is a Taylor-Galerkin finite-element scheme which is third order in space and time [20]. Real-gas thermophysics is consistently implemented in the LES solver using the computationally efficient Peng-Robinson cubic equation of state [21]. Real-gas characteristic boundary conditions [22] and density-dependent transport coefficients [23, 24] are also implemented.

As chemical reaction rates are excessively fast at high pressure, turbulent mixing is here the limiting process. Hence, heat release is computed in the infinitely fast chemistry assumption and taking the presumed shape pdf for the mixture fraction as a beta function, as described in [14]. To prevent spurious heat release in the vicinity of the  $\text{LO}_2$  jet, where the infinitely fast chemistry assumption is not valid due to low temperatures, the reaction rate is set to zero above the  $\rho = 100\text{kg}/\text{m}^3$  threshold.

## 3 Simulated cases and preliminary results

The configuration studied is a single-element injector mounted in an optically accessible square chamber, which has been used in many experimental campaigns on the Mascotte facility (see [25] for a more

complete description of the test bench). Fig. 2 shows the whole computational domain, from the injection unit to the outlet. The chamber length is 400 mm and has a square section of 50 mm side length. Adiabatic slipping walls boundary conditions are used for the chamber and injector walls. In the experimental hot fire tests, the outlet is equipped with a nozzle. In the present simulation, pressure is directly imposed at the outlet, which reduces the computational cost associated with the nozzle. A close-up view of the mesh characteristics near the injector is represented in Fig. 3. It contains approximately 3.5 million cells, with the smallest length of 0.2 mm within the injection unit, to accurately predict the hydrodynamic instability mentioned above. The mesh is then smoothly stretched in the jet development regions from 0.2mm to 1mm, to accurately predict the turbulent flame, and more coarsened in other regions, to a 5mm characteristic length, to minimize the computational cost.

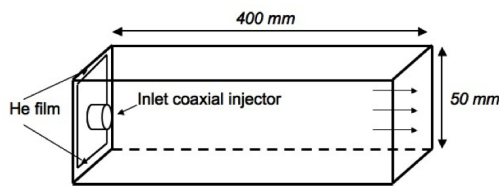


Figure 2: Computational Domain

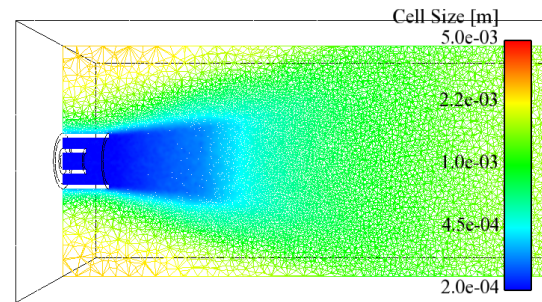


Figure 3: Mesh characteristics

The injection thermodynamic conditions are transcritical : the ambient pressure (60 MPa) is above the critical pressure of the reactants while the injection temperature of the  $\text{LO}_2$  is below its critical temperature. Table 1 details the thermophysical injection conditions. The oxidiser-to-fuel ratio is 2.3.

Species	$T_{inj}$ [K]	$T_C$ [K]	$P_C$ [MPa]	$\rho_{inj}$ [ $\text{kg.m}^{-3}$ ]
$\text{O}_2$	83	154	5.04	1340
$\text{H}_2$	275	33	1.28	5.25

Table 1: Transcritical Injection thermophysical conditions.  $T_{inj}$  is the injection temperature,  $T_C$  and  $P_C$  are the critical temperature and pressure of the species and  $\rho_{inj}$  is the injection density

A preliminary result is shown in Fig. 4, where a high-density 3D isosurface (grey,  $700 \text{ kg.m}^{-3}$ ) showing the dense oxygen core and a 2D cut of the temperature field (color) showing the supercritical jet flame are represented, for both the reference and the recessed case. Work is in progress to analyse the effect of the recess length on the unsteady motions and the flame structure.

Although no hydrodynamic instability has been observed yet, the recessed configuration exhibits a completely different flame shape and length. This is illustrated in Fig. 5(a), where the average oxygen mass fraction along the injector axis is plotted against the axial distance normalized by the oxygen injector inner diameter  $d_{\text{O}_2}$ , for both cases. The recessed injector produces a much shorter flame than the reference case. This difference is due to strain rate intensification induced by confinement effects within the injector, which is visible on Fig. 4. Therefore, recessing the  $\text{LO}_2$  tube modifies heat release and thus wall pressure. The axial wall pressure distribution in the hydrogen injector is represented in Fig. 5(b), which shows a larger pressure drop for the recessed case. However, the recess length has no impact on combustion efficiency: in both cases more than 99.9% of the injected oxygen is burnt before leaving the combustion chamber.

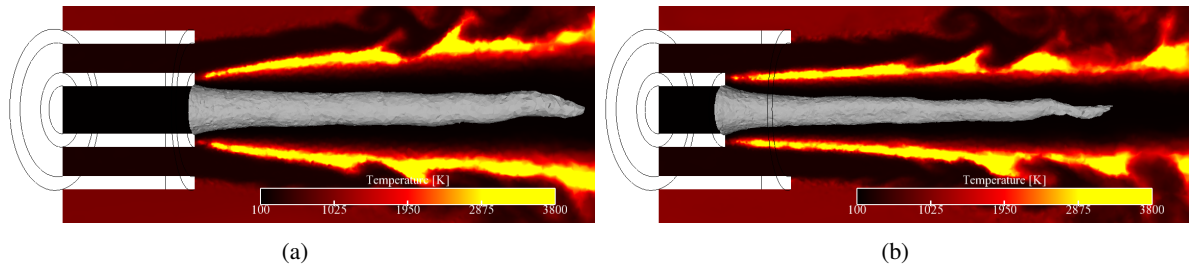


Figure 4: Instantaneous result : high-density 3D isosurface in grey ( $700\text{kg}/\text{m}^3$ ) showing the dense  $LO_2$  core along with a 2D cut of the temperature field (in color) showing the transcritical jet flame for a) the non-recessed injector, b) the recessed-injector.

The authors are now investigating the different mechanisms in detail and are trying to reproduce the hydrodynamic instability observed experimentally by perturbing the initial conditions to trigger an absolute hydrodynamic instability.

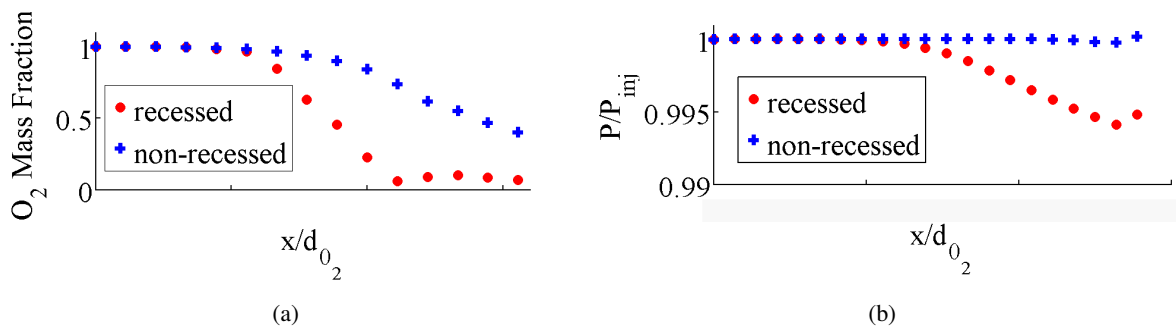


Figure 5: a) Average oxygen mass fraction along the jet axis. b) Axial wall pressure distribution in the hydrogen injector.

## 4 Conclusions

The effect of a design parameter (the recess length) of a coaxial  $LO_2/H_2$  injector is investigated using Large-Eddy Simulation. The recessed configuration is compared to the reference non-recessed configuration, in order to provide more understanding of the injector design effects. The preliminary results presented herein already show large differences on the flame dynamics, mainly due to strain rate intensification within the confinement induced by the recessed injector. Additional analyses and computations using finer meshes are underway to predict the development of the hydrodynamic instability in the recessed injector.

## Acknowledgements

This work is generously supported by Snecma, which is the prime contractor for the European launcher Ariane 5 cryogenic propulsion systems and CNES (Centre National d'Etudes Spatiales), which is the government agency responsible for shaping and implementing France's space policy in Europe.

## References

- [1] O. Haidn and M. Habiballah, "Research on high pressure cryogenic combustion," *Aerospace Science and Technology*, vol. 7, no. 6, pp. 473–491, 2003.
- [2] B. Chehroudi, D. Talley, and E. Coy, "Visual characteristics and initial growth rate of round cryogenic jets at subcritical and supercritical pressures," *Physics of Fluids*, vol. 14, no. 2, pp. 850–861, february 2002.
- [3] M. Oschwald, J. J. Smith, R. Branam, J. Hussong, A. Schik, B. Chehroudi, and D. Talley, "Injection of fluids into supercritical environments," *Combust. Sci. Tech.*, vol. 178, pp. 49–100, 2006.
- [4] J. Bellan, "Supercritical (and subcritical) fluid behavior and modeling: drops, streams, shear and mixing layers, jets and sprays," *Progress in energy and combustion science*, 2000.
- [5] S. Candel, M. Juniper, G. Singla, P. Scoufflaire, and C. Rolon, "Structure and dynamics of cryogenic flames at supercritical pressure," *Combustion Science and Technology*, vol. 178, no. 1, pp. 161–192, 2006.
- [6] L. Cutrone, P. D. Palma, G. Pascazio, and M. Napolitano, "A rans flamelet-progress-variable method for computing reacting flows of real-gas mixtures," *Computers & Fluids*, vol. 39, no. 3, pp. 485 – 498, 2010. [Online]. Available: <http://www.sciencedirect.com/science/article/B6V26-4XFPPW5-1/2/6826e4a2b2d700683b4572d9776aa559>
- [7] A. Benarous and A. Liazid, "H<sub>2</sub>-O<sub>2</sub> supercritical combustion modeling using a CFD code," pp. 139–152, 2009.
- [8] F. Demoulin, S. Zurbach, and A. Mura, "High-Pressure Supercritical Turbulent Cryogenic Injection and Combustion: A Single-Phase Flow Modeling Proposal," *J. Prop. Power*, vol. 25, no. 2, 2009.
- [9] J. Oefelein, "Mixing and combustion of cryogenic oxygen-hydrogen shear-coaxial jet flames at supercritical pressure," *Combust. Sci. Tech.*, vol. 178, no. 1-3, pp. 229–252, 2006.
- [10] N. Zong and V. Yang, "Near-field flow and flame dynamics of LOX/methane shear-coaxial injector under supercritical conditions," *Proceedings of the Combustion Institute*, vol. 31, no. 2, pp. 2309–2317, 2007.
- [11] —, "Cryogenic fluid dynamics of pressure swirl injectors at supercritical conditions," *Physics of Fluids*, vol. 20, p. 056103, 2008.
- [12] T. Schmitt, L. Selle, A. Ruiz, and B. Cuenot, "Large-eddy simulation of supercritical-pressure round jets," *AIAA Journal*, vol. 48, no. 9, pp. 2133–2144, September 2010.
- [13] T. Schmitt, L. Selle, B. Cuenot, and T. Poinot, "Large-Eddy Simulation of transcritical flows," *Comptes Rendus Mécanique*, vol. 337, no. 6-7, pp. 528–538, 2009.
- [14] T. Schmitt, Y. Méry, M. Boileau, and S. Candel, "Large-eddy simulation of oxygen/methane flames under transcritical conditions," *Proceedings of the Combustion Institute*, vol. In Press, Corrected Proof, pp. –, 2010. [Online]. Available: <http://www.sciencedirect.com/science/article/B7GWS-515YH6D-5/2/79a2ea85b542c5e39116dc66d4864023>
- [15] D. Kendrick, G. Herding, P. Scoufflaire, C. Rolon, and S. Candel, "Effects of a recess on cryogenic flame stabilization," *Combust. Flame*, vol. 118, pp. 327–339, 1999.

- [16] B. D. Kim, S. D. Heister, and S. H. Collicott, "Three-dimensional flow simulations in the recessed region of a coaxial injector," *J. Prop. Power*, vol. 21, no. 4, pp. 728–742, 2005.
- [17] N. Gourdain, L. Gicquel, M. Montagnac, O. Vermorel, M. Gazaix, G. Staffelbach, M. García, J.-F. Boussuge, and T. Poinso, "High performance parallel computing of flows in complex geometries - part 1: methods," *Computational Science and Discovery*, vol. 2, no. November, p. 015003 (26pp), 2009. [Online]. Available: [http://www.cerfacs.fr/~cfdbib/repository/TR\\_CFD\\_09\\_117.pdf](http://www.cerfacs.fr/~cfdbib/repository/TR_CFD_09_117.pdf)
- [18] N. Gourdain, L. Gicquel, G. Staffelbach, O. Vermorel, F. Duchaine, J.-F. Boussuge, and T. Poinso, "High performance parallel computing of flows in complex geometries - part 2: applications," *Computational Science and Discovery*, vol. 2, no. November, p. 015004 (28pp), 2009. [Online]. Available: [http://www.cerfacs.fr/~cfdbib/repository/TR\\_CFD\\_09\\_116.pdf](http://www.cerfacs.fr/~cfdbib/repository/TR_CFD_09_116.pdf)
- [19] T. Schönfeld and M. Rudgyard, "Steady and unsteady flows simulations using the hybrid flow solver avbp," *AIAA Journal*, vol. 37, no. 11, pp. 1378–1385, 1999.
- [20] O. Colin and M. Rudgyard, "Development of high-order taylor-galerkin schemes for unsteady calculations," *J. Comput. Phys.*, vol. 162, no. 2, pp. 338–371, 2000.
- [21] D.-Y. Peng and D. B. Robinson, "A new two-constant equation of state," *Industrial & Engineering Chemistry Fundamentals*, vol. 15, pp. 59–64, Feb. 1976. [Online]. Available: [http://pubs3.acs.org/acs/journals/doi/lookup?in\\_doi=10.1021/i160057a011](http://pubs3.acs.org/acs/journals/doi/lookup?in_doi=10.1021/i160057a011)
- [22] N. Okong'o and J. Bellan, "Consistent boundary conditions for multicomponent real gas mixtures based on characteristic waves," *Journal of Computational Physics*, vol. 176, pp. 330–344, 2002.
- [23] T. Chung, M. Ajlan, L. Lee, and K. Starling, "Generalized Multiparameter Correlation for Nonpolar and Polar Fluid Transport Properties," *Industrial & Engineering Chemistry Research*, vol. 27, no. 4, pp. 671–679, 1988.
- [24] T. H. Chung, L. L. Lee, and K. E. Starling, "Applications of kinetic gas theories and multiparameter correlation for prediction of dilute gas viscosity and thermal conductivity," *Industrial & Engineering Chemistry Fundamentals*, vol. 23, pp. 8–13, 1984.
- [25] M. Habiballah, M. Orain, F. Grisch, L. Vingert, and P. Gicquel, "Experimental studies of high-pressure cryogenic flames on the mascotte facility," *Combust. Sci. Tech.*, vol. 178, no. 1-3, pp. 101–128, 2006.